

Supporting Information

Reduction and scavenging of chemically reactive drug metabolites by NAD(P)H:quinone oxidoreductase 1 and NRH:quinone oxidoreductase 2 and variability in hepatic concentrations

Shaleni P. den Braver-Sewradj[#], Michiel W. den Braver[#], Robin M. Toorneman, Stephanie van Leeuwen, Yongjie Zhang, Stefan J. Dekker, Nico P.E. Vermeulen, Jan N.M. Commandeur and J. Chris Vos*

AIMMS-Division of Molecular Toxicology, Department of Chemistry and Pharmaceutical sciences, Vrije Universiteit, De Boelelaan 1108, 1081 HZ Amsterdam, The Netherlands

[#] Authors contributed equally to this study.

* Corresponding author: *Phone:* +31 205987569, *E-mail address:* j.c.vos@vu.nl

Table of Contents:

Table S1 Cytosolic protein contents of 20 liver preparations.

Table S2 Inhibition of recombinant NQO1 and NQO2 by parent drugs used in this study.

Figure S1 Calibration curves of resorufin, recombinant NQO1 activity in resorufin reduction, CB1954 and recombinant NQO2 activity in CB1954 reduction.

Figure S2 Enzyme kinetics of co-substrate NRH oxidation by NQO2.

Figure S3 Inhibition of NQO1 or NQO2 by hydroxydiclofenac

Figure S4 Enzyme kinetics of DCPIP reduction by NQO2 and determination of K_i and mode of inhibition of tacrine

Figure S5 Cytotoxicity of amodiaquine quinone imine in pooled primary human hepatocytes.

Table S1 Cytosolic protein contents of 20 liver preparations.

Donor Preparation	Cytosolic protein content (mg / g liver)
B1327T	375
S1329T	269
S1332T	219
S1334T	198
S1336T	256
S1339T	283
R1341T	251
S1342T	411
S1343T	150
S1344T	297
S1352T	258
S1356T	107
S1399T	253
S1402T	207
S1404T	234
S1405T	383
S1441T	328
S1442T	257
S1446T	293
S1449T	210

Table S2 Inhibition of recombinant NQO1 and NQO2 by parent drugs used in this study. All inhibition experiments were performed in 96-well format in 100 mM KPi buffer containing 2 mM EDTA, 5 mM MgCl₂ and 0.18 mg/ml BSA (pH 7.4). Before starting the reactions, incubations were pre-incubated at 37 °C for 15 min. Concentrations of substrate were chosen at respective Km concentrations, which were previously determined in house in identical format. When 100% inhibition was achieved, K_i values were determined by fitting the data to log(inhibitor) vs. normalized response equation implemented in GraphPad Prism. NQO1 inhibition was investigated by monitoring incubations containing 5 nM NQO1 with 4 μM DCPIP, 100 μM NADPH and inhibitor at 600 nm in time (Bio-Tek Powerwave X 340). NQO2 inhibition was investigated by incubating a) 15 nM NQO2, 25 μM menadione and 100 μM BNAH, b) 50 nM NQO2, 25 μM DCPIP and 100 μM BNAH or c) 75 nM NQO2, 30 μM MTT and 500 μM BNAH which were monitored by a) fluorescence of BNAH (excitation 355 nm and emission 460 nm, Victor 3 Perkin Elmer ¹), b) absorption of DCPIP (600 nm, Bio-Tek Powerwave X 340) or c) absorbance of formazan (product of MTT reduction, 610 nm, Bio-Tek Powerwave X 340). C_{max} values were from literature.²⁻⁶

Enzyme	substrate	Inhibitor	K _i ^a	C _{max} (μM)
NQO1	DCPIP	Dicumarol	170 ± 1 nM	14.5
		Diclofenac	13 ± 1 μM	5
		Mefenamic Acid	40 ± 1 μM	29
		Acetaminophen	> 1 mM	100
		Amodiaquine	> 100 μM	0.11
		Carbamazepine	811 ± 1 μM	38
NQO2	Menadione	Resveratrol	2 ± 0.001 μM	0.3
		Diclofenac	> 1 mM	5
		Mefenamic Acid	66 ± 1 μM	29
		Acetaminophen	> 1 mM	100
		Amodiaquine	160 ± 1 μM	0.11
		Clozapine	746 ± 2 μM	1
	DCPIP	Resveratrol	28 ± 1 μM	0.3
		Diclofenac	> 1 mM	5
		Mefenamic Acid	> 500 μM	29
		Carbamazepine	> 500 μM	38
	MTT	Resveratrol	133 ± 2 μM	0.3
		Diclofenac	> 1 mM	5
		Mefenamic Acid	> 500 μM	29
		Carbamazepine	> 500 μM	38

^a Values are presented as mean ± S.D. (n=3)

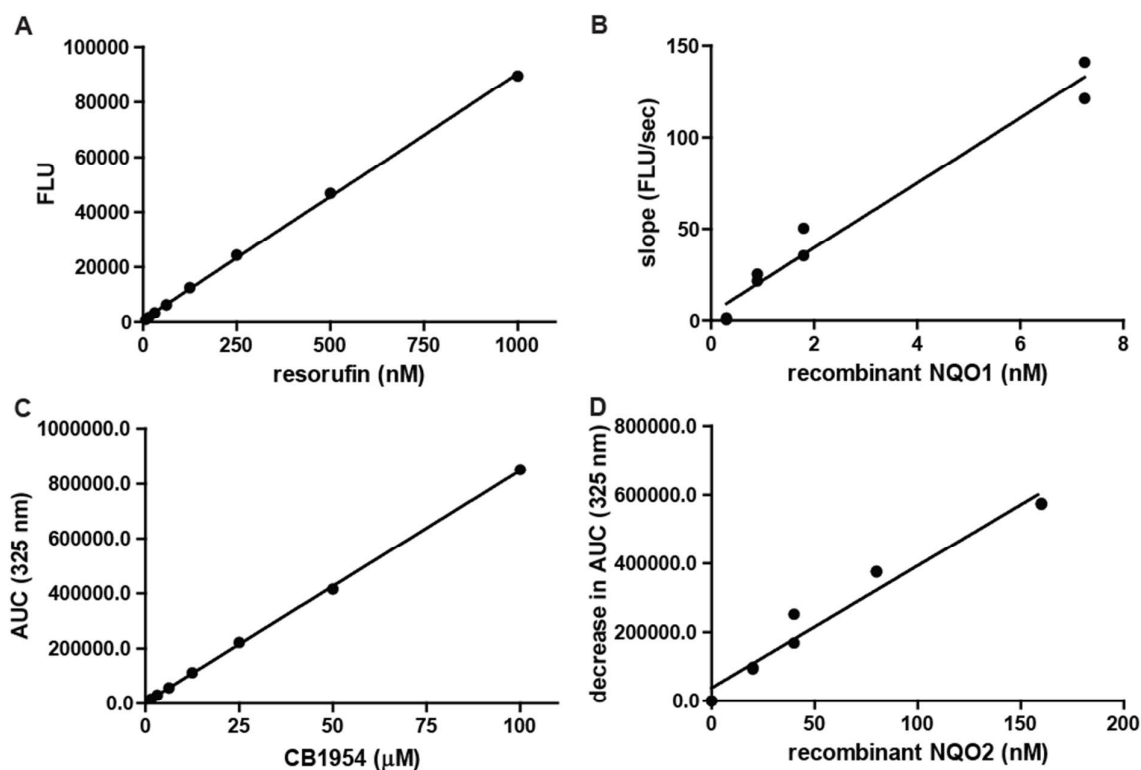


Figure S1 Calibration curves of resorufin (A), recombinant NQO1 activity in resorufin reduction (B), CB1954 (C) and NQO2 activity in CB1954 reduction (D). Incubations were performed as described in materials and methods.

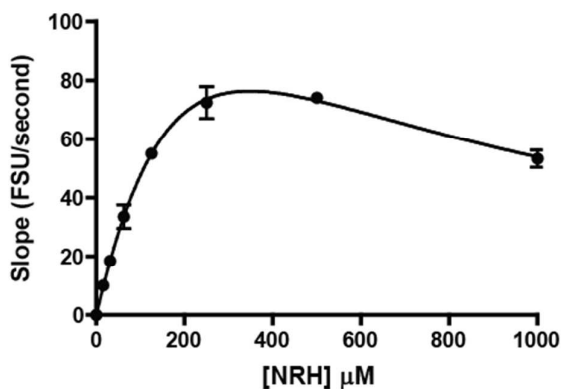


Figure S2 Enzyme kinetics of co-substrate NRH oxidation by NQO2, in presence of the substrate menadione. 100 nM of recombinant NQO2 was pre-incubated with NRH (0-1000 μ M) in 100 mM KH_2PO_4 buffer containing 2 mM EDTA, 5 mM MgCl_2 and 0.18 mg/ml BSA (pH 7.4) for 15 minutes at 37 $^\circ\text{C}$ in a 96 well plate. Reactions were started by addition of 100 μ M (final) menadione and depletion of NRH was measured monitored in time for 2 min (excitation 355 nm and emission 460 nm, Victor 3 Perkin Elmer ¹). The y-axis shows the decrease of arbitrary fluorescence units (FSU)/second. Data is corrected for chemical reduction and represent means of triplicates. Data is

fitted in Graphpad Prism (version 5.0) using the substrate inhibition model. Data represents the mean and S.D. of triplicates.

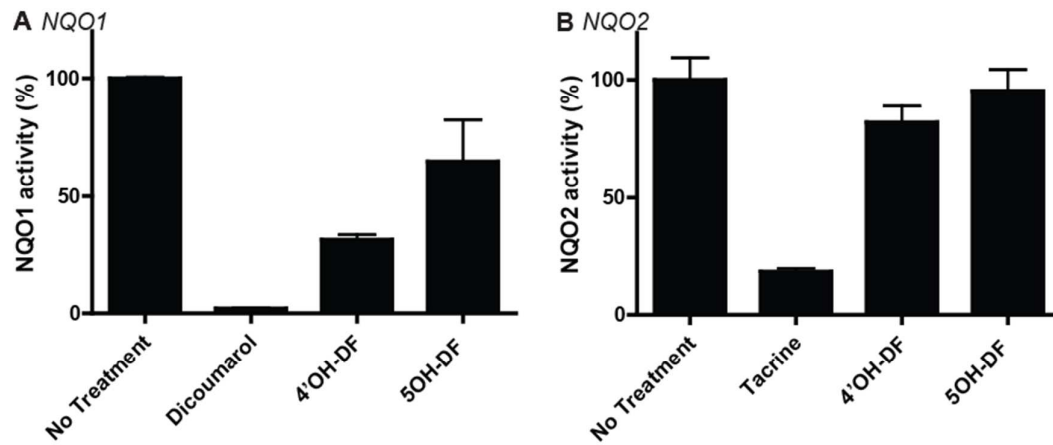


Figure S3 Inhibition of NQO1 or NQO2 by hydroxydiclofenac. Quinone reductases (5 nM NQO1 or 50 nM NQO2) were pre-incubated with 100 μ M co-substrate (NADPH for NQO1, NRH for NQO2) with or without inhibitor (50 μ M) in 100 mM KPi buffer containing 2 mM EDTA, 5 mM $MgCl_2$ and 0.18 mg/ml BSA (pH 7.4) for 15 minutes at 37 $^{\circ}C$ in a 96 well plate. Reactions were started by addition of 25 μ M (final) DCPIP. DCPIP reduction was followed in time at 600 nm, for 2 min (Bio-Tek Powerwave X 340). Abbreviations: 4'OH-DF, 4'hydroxydiclofenac; 5OH-DF, 5-hydroxydiclofenac. Data represents the average and range of duplicates.

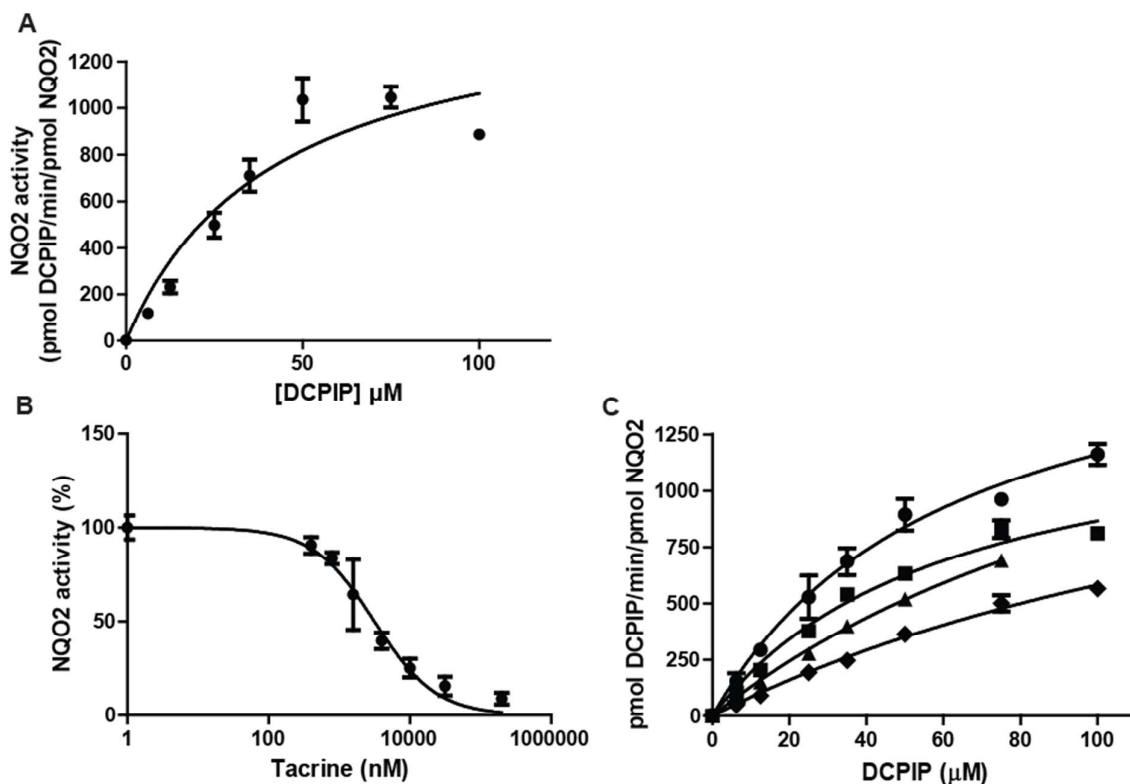


Figure S4 Enzyme kinetics of DCPIP reduction by NQO2 (A) and determination of K_i (B) and mode of inhibition (C) of tacrine. Incubations were performed in 96 well format in 100 mM KPi containing 2 mM EDTA, 5 mM MgCl_2 and 0.18 mg/ml BSA. Enzyme kinetics were investigated by pre-incubation of 50 nM of NQO2 with 100 μM BNAH for 15 minutes at 37 °C. Reactions were started by addition of DCPIP (6.25-100 μM) and absorbance at 600 nm was followed in time (Bio-Tek Powerwave X 340). The K_m value (25 μM) was determined by fitting the data to the Michaelis Menten equation in Graphpad Prism (version 5.0). The K_i (A) and mode of inhibition (B) was investigated under similar conditions. For determination of the K_i (A, 3 ± 1 μM) tacrine (0-200 μM) was included in the pre-incubation. Data was fitted to $\log(\text{inhibitor})$ vs. normalized response equation implemented in GraphPad Prism (version 5.0). For the mode of inhibition (B) tacrine was excluded (circles) or included at its IC25 (squares, 1 μM), IC50 (triangles, 3 μM) or IC75 (diamonds, 7 μM) concentrations. Data was analyzed using the Menten equation in Graphpad Prism (version 5.0). Both K_m and V_{max} changed in presence of tacrine, identifying tacrine as a mixed-type inhibitor. Data represents the mean and S.D. of triplicates.

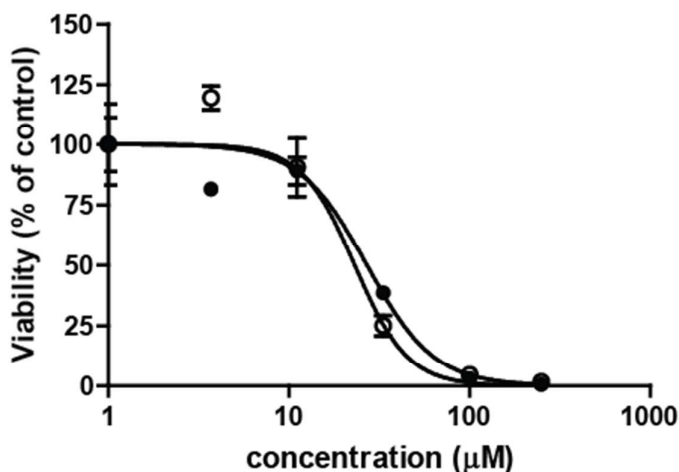


Figure S5 Cytotoxicity of amodiaquine quinone imine in pooled primary human hepatocytes (P2109A, KalyCell). Primary human hepatocytes were incubated in suspension as described before.^{7,8} Cells were exposed to selected concentrations of amodiaquine quinone imine (0.1% final DMF) in presence (open circles) or absence (closed circles) of 20 µM dicoumarol. Dicoumarol was pre-incubated for 15 minutes. Following an incubation with amodiaquine quinone imine of 2 hours, cytotoxicity was assessed using reduction of resazurin as viability marker as described before.⁷ IC₅₀ values were 23 µM and 27 µM (in presence or absence of dicoumarol, respectively) and were not significantly different. Data represents the average and range of duplicates.

References:

- (1) Long, D. J., Iskander, K., Gaikwad, A., Arin, M., Roop, D. R., Knox, R., Barrios, R., and Jaiswal, A. K. (2002) Disruption of dihydronicotinamide riboside:quinone oxidoreductase 2 (NQO2) leads to myeloid hyperplasia of bone marrow and decreased sensitivity to menadione toxicity. *J. Biol. Chem.* 277, 46131–9.
- (2) Verner, M., Magher, T., and Haddad, S. (2010) High concentrations of commonly used drugs can inhibit the in vitro glucuronidation of bisphenol A and nonylphenol in rats. *Xenobiotica.* 40, 83–92.
- (3) Sinou, V., Malaika, L. T. M., Taudon, N., Lwango, R., Alegre, S. S., Bertaux, L., Sugnaux, F., Parzy, D., and Benakis, A. (2009) Pharmacokinetics and pharmacodynamics of a new ACT formulation: Artesunate/Amodiaquine (TRIMALACT) following oral administration in African malaria patients. *Eur. J. Drug Metab. Pharmacokinet.* 34, 133–142.
- (4) Sergides, C., Chirilă, M., Silvestro, L., Pitta, D., and Pittas, A. (2016) Bioavailability and safety study of resveratrol 500 mg tablets in healthy male and female volunteers. *Exp. Ther. Med.* 11, 164–170.
- (5) MacHeras, P. E., and Reppas, C. I. (1986) Studies on drug-milk freeze-dried formulations I:

Bioavailability of sulfamethizole and dicumarol formulations. *J. Pharm. Sci.* 75, 692–696.

(6) Sramek, J. J., Anand, R., Hartman, R. D., Schran, H. F., Hourani, J., Barto, S., Wardle, T. S., Shiovitz, T. M., and Cutler, N. R. (1999) A Bioequivalence Study of Brand and Generic Clozapine in Patients with Schizophrenia. *Clin. Drug Investig.* 17, 51–58.

(7) Richert, L., Baze, A., Parmentier, C., Gerets, H. H. J., Sison-Young, R., Dorau, M., Lovatt, C., Czich, A., Goldring, C., Park, B. K., Juhila, S., Foster, A. J., and Williams, D. P. (2016) Cytotoxicity evaluation using cryopreserved primary human hepatocytes in various culture formats. *Toxicol. Lett.* 258, 207–215.

(8) Alexandre, E., Viollon-Abadie, C., David, P., Gandillet, A., Coassolo, P., Heyd, B., Manton, G., Wolf, P., Bachellier, P., Jaeck, D., and Richert, L. (2002) Cryopreservation of adult human hepatocytes obtained from resected liver biopsies. *Cryobiology* 44, 103–13.